Identification, expression, and functional analyses of a thylakoid ATP/ADP carrier from Arabidopsis

Sophie Thuswaldner, Jens O. Lagerstedt, Marc Rojas-Stütz, Karim Bouhidel, Christophe Der, Nathalie Leborgne-Castel, Arti Mishra, Francis Marty, Benoît Schoefs, Iwona Adamska, et al.

THE JOURNAL OF BIOLOGICAL CHEMISTRY VOL. 282, NO. 12, pp. 8848–8859, March 23, 2007

Identification, Expression, and Functional Analyses of a Thylakoid ATP/ADP Carrier from *Arabidopsis*[*] [S]

Received for publication, September 26, 2006, and in revised form, December 22, 2007 Published, JBC Papers in Press, January 29, 2007, DOI 10.1074/jbc.M609130200

Sophie Thuswaldner[‡], Jens O. Lagerstedt[§1,2], Marc Rojas-Stütz[¶1], Karim Bouhidel[‖], Christophe Der[‖], Nathalie Leborgne-Castel[‖], Arti Mishra[‡‡], Francis Marty[‖], Benoît Schoefs[‖], Iwona Adamska[¶], Bengt L. Persson[§], and Cornelia Spetea[‡3]

From the [‡]Division of Cell Biology and [‡‡]Department of Physics, Chemistry and Biology, Linköping University, SE-581 85 Linköping, Sweden, [§]Department of Chemistry and Biomedical Sciences, Kalmar University, SE-391 82 Kalmar, Sweden, [¶]Department of Physiology and Plant Biochemistry, University of Konstanz, D-78457 Konstanz, Germany, and [‖]UMR Plante-Microbe-Environnement CNRS 5184/Institut National de la Recherche Agronomique1088, Université de Bourgogne, BP 47870, F-21078 Dijon Cedex, France

In plants the chloroplast thylakoid membrane is the site of light-dependent photosynthetic reactions coupled to ATP synthesis. The ability of the plant cell to build and alter this membrane system is essential for efficient photosynthesis. A nucleotide translocator homologous to the bovine mitochondrial ADP/ATP carrier (AAC) was previously found in spinach thylakoids. Here we have identified and characterized a thylakoid ATP/ADP carrier (TAAC) from *Arabidopsis*. (*i*) Sequence homology with the bovine AAC and the prediction of chloroplast transit peptides indicated a putative carrier encoded by the At5g01500 gene, as a TAAC. (*ii*) Transiently expressed TAAC-green fluorescent protein fusion construct was targeted to the chloroplast. Western blotting using a peptide-specific antibody together with immunogold electron microscopy revealed a major location of TAAC in the thylakoid membrane. Previous proteomic analyses identified this protein in chloroplast envelope preparations. (*iii*) Recombinant TAAC protein specifically imports ATP in exchange for ADP across the cytoplasmic membrane of *Escherichia coli*. Studies on isolated thylakoids from *Arabidopsis* confirmed these observations. (*iv*) The lack of TAAC in an *Arabidopsis* T-DNA insertion mutant caused a 30–40% reduction in the thylakoid ATP transport and metabolism. (*v*) TAAC is readily expressed in dark-grown *Arabidopsis* seedlings, and its level remains stable throughout the greening process. Its expression is highest in developing green tissues and in leaves undergoing senescence or abiotic stress. We propose that the TAAC protein supplies ATP for energy-dependent reactions during thylakoid biogenesis and turnover in plants.

Chloroplasts perform oxygenic photosynthesis in algae and plants and have evolved by endosymbiosis from cyanobacteria. Chloroplasts have two distinct membrane systems, the double envelope surrounding the organelle and an internal membrane system named thylakoids. The envelope membrane represents the interface between the cytoplasm and chloroplast stroma, whereas the thylakoid membrane separates the stroma and the lumenal space. Altogether ~800 membrane proteins have been identified by proteomics in the envelope and thylakoid membranes of *Arabidopsis thaliana* (for reviews, see Refs. 1 and 2). As expected, the main function for the identified envelope proteins was transport of ions and metabolites, whereas photosynthesis was attributed to most of the identified thylakoid proteins. The major protein complexes in thylakoids are photosystems (PS)[4] I and II, the cytochrome b_6f complex, and the proton-translocating ATP synthase. These photosynthetic complexes contain not only proteins but also pigments and other cofactors. Their assembly, activity, and removal require a large number of auxiliary, regulatory, and transport proteins (3, 4). Many biochemical reports pointed to the existence of transport activities in the thylakoid membrane, such as calcium transport (5), copper transport (6), anion channels (7), cation channels (8, 9), and nucleotide transport (10). Only the thylakoid copper transporter was identified at the genetic level in *Arabidopsis* (11). No hydrophobic proteins related to the above-mentioned transport activities were identified in the previous proteomic works on *Arabidopsis* thylakoid membranes (for a review, see Ref. 2). Therefore, genetic strategies are required for identification and elucidation of their role in optimal function of the thylakoid.

ATP is produced during the light-dependent photosynthetic reactions on the stromal side of the thylakoid membrane. Besides its utilization during CO_2 fixation in the stroma, ATP drives many energy-dependent processes in thylakoids, including protein phosphorylation, folding, import, and degradation.

* This work was supported by the Swedish Research Council (to C. S. and B. L. P.), the Graduate Research School in Genomics and Bioinformatics and Hagberg Foundation (to C. S.), the Human Frontier Science Organization (to B. L. P.), Deutsche Forschungsgemeinschaft and Konstanz University (to I. A.), and the French Ministère de l'Education Nationale de l'Enseignement Supérieur et de la Recherche, the Institut National de la Recherche Agronomique, and the CNRS (Dijon group). The costs of publication of this article were defrayed in part by the payment of page charges. This article must therefore be hereby marked "*advertisement*" in accordance with 18 U.S.C. Section 1734 solely to indicate this fact.

[S] The on-line version of this article (available at http://www.jbc.org) contains supplemental material including Figs. S1–S4 and Table S1.

[1] These authors equally contributed to this work.

[2] Present address: Depts. of Biochemistry and Molecular Medicine, and Internal Medicine, University of California, School of Medicine, Davis, CA 95616.

[3] To whom correspondence should be addressed. Tel.: 46-13-225788; Fax: 46-13-224314; E-mail: cornelia.spetea@ibk.liu.se.

[4] The abbreviations used are: PS, photosystem; AAC, ADP/ATP carrier; CCCP, *m*-chlorocarbonyl cyanide phenylhydrazone; Chl, chlorophyll; GFP, green fluorescent protein; IPTG, isopropyl 1-thio-β,D-galactopyranoside; MCF, mitochondrial carrier family; NDPK, nucleoside diphosphate kinase; TAAC, thylakoid ATP/ADP carrier; bAAC, bovine AAC protein; TLC, thin layer chromatography; TMD, transmembrane domain; Tricine, *N*-[2-hydroxy-1,1-bis(hydroxymethyl)ethyl]glycine; WT, wild type.

Alternatively, ATP is transported across the membrane into the lumenal space and converted to GTP by a nucleoside diphosphate kinase, NDPK3 (10). There are also several recent indications for the presence of phosphorylated proteins in the thylakoid lumen of green algae and plants, as provided by mass spectrometry analyses (12, 13). The transport of ATP across the thylakoid membrane proceeds via a nucleotide-binding protein of 36.5 kDa (10). This protein is homologous to the bovine mitochondrial ADP/ATP carrier (AAC), which is the most studied member of the mitochondrial carrier family (MCF, Prosite PS50920). The structure of the bovine AAC was solved by x-ray crystallography at 2.2 Å of resolution in the presence of carboxyatractyloside (14). In *Arabidopsis* there are three genes encoding for mitochondrial AACs (15). All three proteins were identified in the mitochondrial proteome (16) and were shown to transport adenine nucleotides when expressed in heterologous system (17). The protein(s) responsible for the thylakoid ATP transport activity (10) have not yet been isolated or identified at the genetic level.

In this work we provide computer-based and experimental evidence that the product of the *Arabidopsis* At5g01500 gene is a thylakoid ATP/ADP carrier (TAAC). In a previous proteomic study this protein was concluded to be localized in the chloroplast (inner) envelope (18). Here we demonstrate a major thylakoid and a minor envelope location for the TAAC protein. Our studies also show that TAAC is readily expressed in *Arabidopsis* dark-grown seedlings and appears to be needed for both synthesis of photosynthetic complexes during greening and for their recycling during senescence and stress.

EXPERIMENTAL PROCEDURES

Plant Material—Arabidopsis (*A. thaliana* cv. Columbia) plants were grown hydroponically (19) or on soil (for expression studies) at 120 μmol of photons m^{-2} s^{-1} and 22 °C with 8-h light/16-h dark cycles. For localization using immunogold, *Arabidopsis* cv. Wassilewskaja was grown on soil. For transient expression studies, tobacco (*Nicotiana tabacum* cv. Xanthi) plants were grown on Murashige Skoog medium at 100 μmol of photons m^{-2} s^{-1} and 24 °C under a 16-h light/8-h dark photoperiod.

Arabidopsis (cv. Wassilewskaja) seeds of the T-DNA insertion line FLAG 443D03 (*taac* mutant, supplemental Fig. S1*A*) were obtained from PublicLines at Institut National de la Recherche Agronomique. For screening of homozygous mutant plants, genomic DNA isolated from wild type (WT) and the *taac* mutant was analyzed by two sets of PCR reactions using gene-specific forward 5′-AGAACAACGTGTCGTCGAATC-3′ and reverse 5′-CAACACCATTCTTTCCAAAAGG-3′ primers and the T-DNA left border 5′-TGGTTCACGTAGTGGGCCATCG-3′ primer (supplemental Fig. S1*B*). Homozygoty was confirmed in the next generation.

Structural Analyses—Homology and orthology searches using BLAST were performed in MIPS, TIGR, and Cyanobase. Prediction of intracellular location and membrane topology were performed using TargetP, the PPDB data base, and a package of programs at ARAMEMNON website. The amino acid sequences were aligned with ClustalW.

A structural homology model of the *Arabidopsis* TAAC protein was built from its amino acid sequence by use of several local structure and fold recognition methods at the MetaServer (20). The established structure of the protein with the highest scores (bovine AAC; PDB code 1okc A) was used as template, and the comparison was done using the Swiss-Model program (21). The calculated three-dimensional model was obtained by optimally satisfying spatial restraints derived from the 3D-Jury sequence alignment. Analysis of the TAAC structural model was performed by use of the DeepView/Swiss-PdbViewer program and also by use of Insight II software (Version 2005) on the Octane work station by Silicon Graphics. The structural model shown (Fig. 1*D*) was produced by use of the latter.

Transient Expression of a TAAC-GFP Fusion Construct and Microscope Analysis—The entire coding region of the *TAAC* gene was amplified by PCR using an *Arabidopsis* CD4–14 cDNA library (22) and subcloned into the expression vector pDR303. In the resulting pNL1500 plasmid the *TAAC* sequence was fused in-frame to the 5′-end of a green fluorescent protein (GFP) coding sequence and placed under the control of the transcriptional 35S promoter from the cauliflower mosaic virus (CaMV35S). This plasmid was introduced into tobacco leaf protoplasts by electroporation. After 24 h of incubation in darkness, protoplasts were imaged using a confocal laser-scanning microscope. The detailed protocols for construct design, protoplast isolation, electroporation, and microscope analysis are described under supplemental "Experimental Procedures."

Chloroplast Membrane Preparations—Arabidopsis chloroplasts were prepared (23) and lysed in 50 mM Tricine/KOH (pH 7.6) and 5 mM $MgCl_2$ (Tricine buffer) for 10 min on ice. Thylakoids and envelope membranes were purified from the lysate by centrifugation at 113,000 × *g* for 1 h on sucrose step gradient (0.6, 0.93, 1.2, and 1.5 M sucrose). Thylakoids were collected at the 1.2/1.5 M interface, diluted with Tricine buffer, and centrifuged at 10,000 × *g* for 10 min. Envelope membranes were collected at the 0.93/1.2 M interface, diluted with Tricine buffer, and centrifuged at 10,000 × *g* for 10 min (to discard thylakoid vesicles) followed by 150,000 × *g* for 30 min. The thylakoids and envelope membranes were finally resuspended in Tricine buffer supplemented with 0.3 M sucrose. Chlorophyll (Chl) and protein concentrations were determined as described (24, 25). For topology studies, thylakoid membranes (0.2 mg of Chl ml^{-1}) were treated with 1 M NaCl or 0.1 or 1% (w/v) Triton X-100 for 30 min on ice in darkness followed by centrifugation at 150,000 × *g* for 30 min. Both supernatants and pellets were analyzed by Western blotting.

Protein Analysis—SDS/PAGE and Western blotting were performed as described (26). An anti-TAAC antibody was produced in rabbit against a peptide corresponding to the last 15 residues at C terminus of the *Arabidopsis* protein and purified by affinity chromatography (Innovagen, Lund, Sweden). Where indicated, antibodies against the 110-kDa protein of the translocon of the chloroplast inner envelope membrane (TIC110, a gift from Prof. J. Soll), a light-harvesting Chl *a/b*-binding protein of PSII (Lhcb2, Agrisera, Umeå, Sweden), and an anti-Xpress antibody (Invitrogen) were also used.

Immunogold Electron Microscopy—Arabidopsis rosette leaves were thinly diced and fixed overnight. After blocking in

1% (w/v) bovine serum albumin, the grids were incubated with the anti-TAAC antibody followed by incubation with goat anti-rabbit serum conjugated with colloidal gold particles, staining, and electron microscopy as earlier described (27). Detailed protocols are given under supplemental "Experimental Procedures."

Cloning, Heterologous Expression, and Purification of a Recombinant TAAC Protein—All DNA manipulations, including PCR, restriction digestion, agarose gel electrophoresis, ligation, and transformation into *Escherichia coli* (*E. coli*) DH5α, were performed by standard procedures (28). The *Arabidopsis TAAC* gene was PCR-amplified with oligonucleotides designed to exclude the first 177 base pairs of the gene (corresponding to the predicted transit peptide), cloned, and recombined as a fusion construct with an N-terminal hexahistidine tag followed by Xpress epitope and a C-terminal FLAG epitope (DYKDDDDK) into a pTrcHisB plasmid for expression in *E. coli*. Such a set-up has previously been employed to purify another membrane-embedded protein (29). The detailed protocols are given under supplemental "Experimental Procedures."

Uptake of Radioactive ATP and ADP into E. coli Cells—For uptake experiments cells transformed with the *TAAC*-expressing plasmid (or control expression plasmid) were induced with isopropyl 1-thio-β,D-galactopyranoside (IPTG) for 6 h in Terrific Broth medium supplemented with 10 mM malate and 10 mM pyruvate (17). Uptake experiments were carried out according to Haferkamp *et al.* (17) and Tjaden *et al.* (30) with a few modifications. Cells (30 μl, 100 μg μl^{-1}) were incubated in 50 mM phosphate buffer (pH 7.0) containing 50 μM [α-^{32}P]ATP (500 mCi/mmol; 1 μCi = 37 kBq, Amersham Biosciences) or [α-^{32}P]ADP, prepared according to Tjaden *et al.* (30) at 30 °C for the indicated time periods. Where indicated, the uptake experiments were carried out in the presence of 2.5 mM various nonlabeled nucleotides. For determination of the transport affinity (K_m) and the maximal rate (V_{max}), uptake of a range of concentrations (0–250 μM) of [α-^{32}P]ATP or [α-^{32}P]ADP was carried out in *E. coli* cells preincubated or not with 100 μM *m*-chlorocarbonyl cyanide phenylhydrazone (CCCP) for uncoupling. The cells were thereafter quickly filtrated through a 0.45-μm filter (Pall, New York) under vacuum and washed three times with 1 ml of ice-cold phosphate buffer. The radioactivity retained on the filters was quantified in 3.5 ml of water using scintillation spectrometry. Back exchange experiments were carried out essentially as previously described (17, 30). The detailed protocol is provided under supplemental "Experimental Procedures."

Uptake of Radioactive ATP into Thylakoids and Assay of NDPK Activity—*Arabidopsis* thylakoids (30 μl, 0.3 μg of Chl μl^{-1}) were incubated in Tricine buffer containing 10 μM [α-^{32}P]ATP in darkness at 22 °C for the indicated periods of time. In some experiments the uptake was carried out using 0–50 μM [α-^{32}P]ATP or in the presence of 1 mM nonlabeled nucleotides. The thylakoids were washed twice and recovered by rapid centrifugation (45 s, 13,000 × *g*), and their radioactivity was counted in 1 ml of water. Control experiments in the presence of 10 mM nonlabeled ATP indicated 10% nonspecific binding. This value was substracted from all measured activities. Back exchange experiments were performed essentially as described for *E. coli*. Details are given under supplemental "Experimental Procedures." NDPK activity was assayed as the amount of [γ-^{32}P]GTP produced from 1 mM [γ-^{32}P]ATP (12.5 Ci/mmol) and 1 mM GDP, as described (10).

RNA Extraction and Northern Blot Analysis—Total RNA was extracted from frozen *Arabidopsis* tissues using TRIzol® and Plant RNA Purification Reagent (Invitrogen) or RNeasy Kit (Qiagen, Germantown, CA) according to the manufacturer's instructions. Equal amounts (5–10 μg) of RNA were separated on a 1.2% (w/v) denaturating formaldehyde/agarose gel and transferred to a positively charged nylon membrane (Roche Applied Science) (28). The *TAAC* probe was obtained by PCR amplification of a 430-bp fragment using the At5g01500 cDNA as template and the digoxigenin (DIG)-labeled deoxynucleotide mixture (Roche Applied Science). The following PCR primers were used: forward, 5′-GGCACCGCTTGACCGAATAA, and reverse, 5′-AAGCGAAGGACCTAGACCGTTGTA. Hybridization was carried out according to the instructions in the DIG-Nonradioactive Nucleic Acid Labeling and Detection System (Roche Applied Science).

RESULTS

Structural Analyses of the TAAC Protein—Similarity search with the amino acid sequence of the bovine AAC against the *Arabidopsis* protein data base combined with prediction of transit peptides revealed six plastid MCF members, which is in line with previously published data (31). Among them, the product of the At5g01500 gene (MIPS code for *TAAC*) with a putative carrier function corresponded in size to the previously reported nucleotide thylakoid transporter (10). The coding region of the At5g01500 gene obtained by screening of an *Arabidopsis* cDNA library (22) confirmed the exon assignment in the MIPS data base. In the same data base five expressed sequence tags (ESTs) were found for *Arabidopsis TAAC*, indicating that the gene is transcriptionally active.

The encoded *Arabidopsis* TAAC protein contains 415 amino acids and an N-terminal chloroplast transit peptide (amino acids 1–59), as indicated by TargetP (score 0.764, RC3) (Fig. 1*A*). Using advanced bioinformatics analysis for intra-chloroplast protein sorting (32), a low cysteine content (0.07%) and a negative GRAVY index (-0.079) were determined (data extracted from PPDB) that are in favor of a thylakoid rather than envelope location for this putative protein. Nevertheless, it was annotated as an envelope protein due to its high hydrophobicity, high isoelectric point, and putative carrier function (18). Notably, two proteomic studies disagree on the envelope localization of the At5g01500 gene product (18, 33).

The mature form shows 28% identity (43% similarity) to the bovine AAC protein (bAAC). The TAAC termini are 50 (N) and 30 (C) residues, respectively, longer than the corresponding regions in bAAC and are rich in both positively and negatively charged residues (Fig. 1*A*). The presence of a five-glycine repeat in the middle of the N terminus indicates that this region may undergo large conformational changes that could regulate TAAC activity. A ring of four well conserved positively charged residues (Lys-22, Arg-79, Tyr-186, and Arg-279 in bAAC) was proposed to act as a selectivity filter for adenine nucleotides in all AACs (14, 34). The alignment (Fig. 1*A*) shows that these

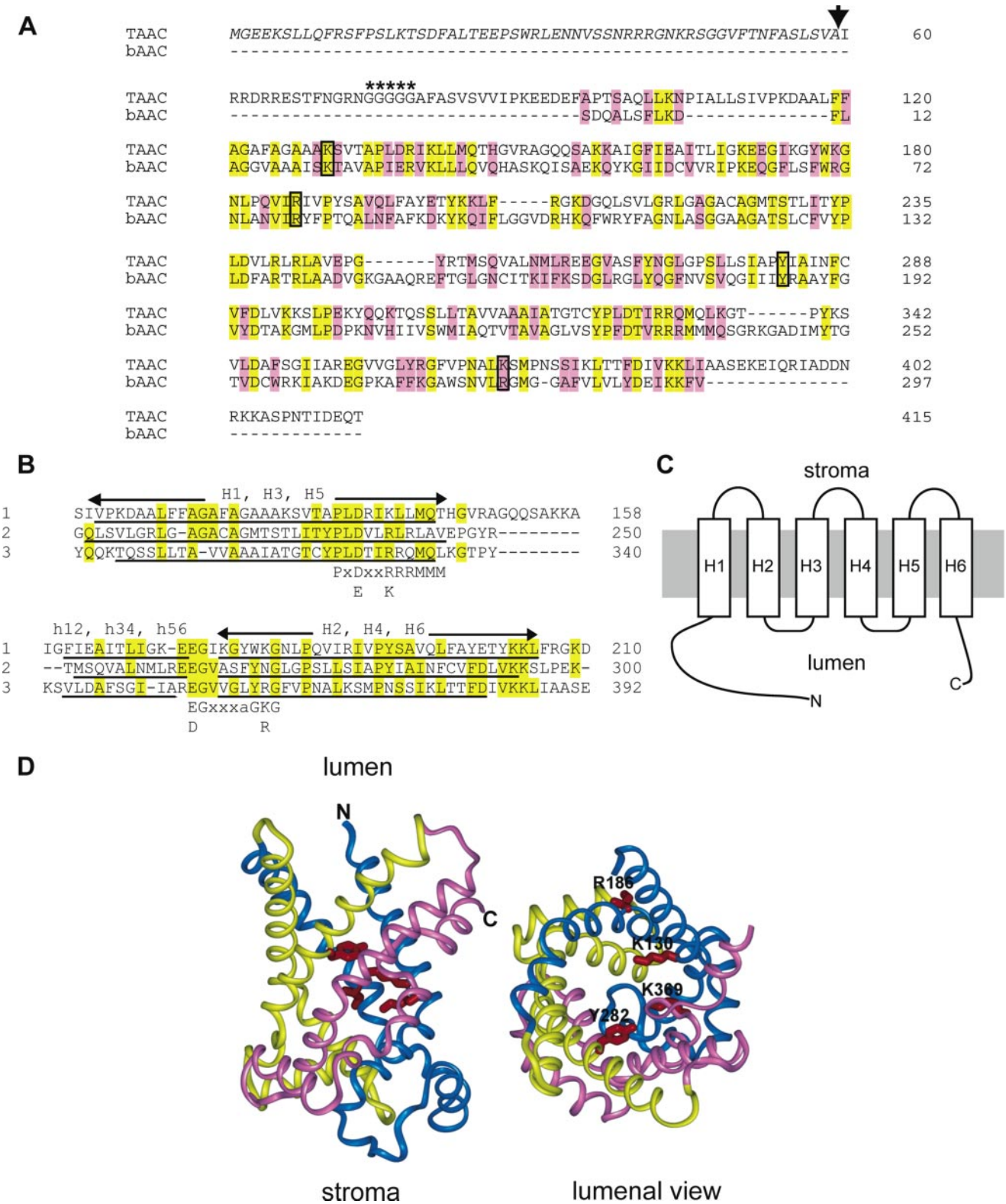

FIGURE 1. ***In silico* analyses of the *Arabidopsis* TAAC protein.** *A*, sequence alignment of the TAAC precursor protein (TrEMBL Q9M024) with the bAAC (Swiss-Prot P02722), as performed by ClustalW. The transit peptide cleavage site of TAAC (as predicted by TargetP) is marked by an *arrow*. Identical and conserved residues are indicated in *yellow* and *pink*, respectively. A glycine repeat is highlighted (*). Four residues composing the selectivity filter are marked by *borderlines*. *B*, alignment of three repeated homologous regions in the TAAC amino acid sequence. Identical residues between the repeats are *highlighted* in *yellow*. The putative TMDs (*H1–H6*) and the short amphipatic helices (*h12*, *h34*, *h56*) are *underlined*. The consensus MCF motif and the AAC signature are indicated *below* the *alignment*. *C*, folding model of the TAAC protein, as based on the membrane topology of bAAC. Boxes H1–H6 denote the putative TMDs. *N* and *C* denote the protein termini, both located on the lumenal side of the thylakoid membrane. *D*, structural homology model of TAAC (residues 110–384), as based on the x-ray structure of bAAC (PDB 1okc A). The three repeats underlined in *B* are shown in *blue* (residues 110–207), *yellow* (residues 208–300), and *pink* (residues 301–384). The side chains of the selectivity filter residues marked with borderlines in *A* are *highlighted* in *red*.

residues are also conserved in TAAC (Lys-130, Arg-186, Tyr-282, Lys-369), suggesting a possible substrate preference for adenine nucleotides. As was found in all MCF members, TAAC contains three repeated homologous regions, with highly conserved consensus sequences (Fig. 1*B*). The unique AAC signature (RRRMMM) in the third repeat region is only partially conserved in TAAC (RRqMql, where the lowercase letters indicate nonconserved residues), as in the case of two other AACs (34). The relevance of this signature for binding and/or transport of adenine nucleotides is not clearly understood. Nevertheless, the detailed analysis of the bovine AAC x-ray structure indicated that only the first two arginines (also conserved in TAAC) interact with carboxyatractyloside (34).

Various software tested at the ARAMEMNON website indicated zero to six transmembrane domains (TMDs) for the TAAC protein. The reason for this large variability is the presence of many charged residues as well as conserved prolines in the putative TMDs of this type of transport protein, unusual features for which various software is more or less sensitive, as suggested previously (32). Six TMDs have been revealed in the crystal structure of the bovine AAC (14). Therefore, we have used the alignment with the bovine carrier (Fig. 1*A*) as basis for the presence of six TMDs in the TAAC structure (Fig. 1*B*). In the folding model of the TAAC protein (Fig. 1*C*), the TMDs are connected by three loops on the stromal side and two loops on the lumenal side. The stromal loops contain amphipatic helices (*h12*, *h34*, and *h56*, Fig. 1*B*). For the mitochondrial AAC, the N and C termini are in the intermembrane space, and the adenine nucleotide-binding site is on the matrix side of the membrane, where ATP is synthesized. Taking into account that in chloroplasts ATP is synthesized on the stromal side of the thylakoid membrane and is transported from the stroma into the thylakoid lumen (10), the N and C termini of the TAAC protein are expected to be located on the lumenal side of membrane (Fig. 1*C*).

The TAAC amino acid sequence was analyzed for structural homologues at the MetaServer (20). As expected, substantial structural similarities to the bovine AAC (PDB 1okc A) were identified, and a highly significant 3D-Jury homology score (140.2) was provided. The presented structural homology model of TAAC (Fig. 1*D*) is limited to amino acid residues 110–384, excluding the large N and C termini, which have no correspondence in the bovine AAC. Like the bovine protein, the overall structure is basket-shaped, with a closure on the stromal side and opening on the lumenal side (Fig. 1*D*, side view). The backbone exhibits a pseudo-3-fold symmetry due to the presence of three repeated homologous domains. The TMDs form a cavity that enters deeply into the protein, and the four indicated residues making up the selective filter (Lys-130, Arg-186, Tyr-282, Lys-369) surround the bottleneck of the cavity (Fig. 1*D*, lumenal view). Taken together, the structural analyses indicate that the product of the At5g01500 gene possesses a chloroplast transit peptide as well as the characteristic sequence features of a MCF and AAC member.

In Vivo and in Vitro Localization Studies of the TAAC Protein—The targeting of a TAAC-GFP construct was investigated in tobacco leaf protoplasts (Fig. 2*A*). As shown in the merge image (Fig. 2*D*), GFP fluorescence (Fig. 2*B*) and Chl red autofluorescence (Fig. 2*C*) colocalized. These data show that TAAC is efficiently targeted to the chloroplast. However, no information about the intra-chloroplast localization could be obtained.

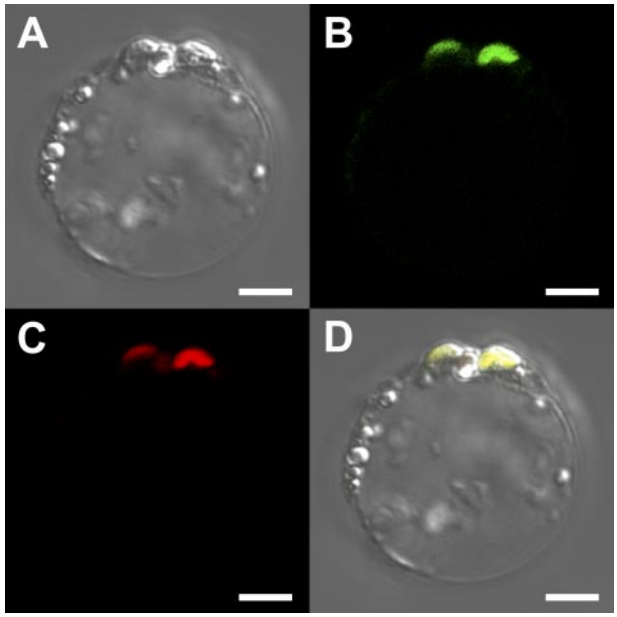

FIGURE 2. **Targeting of the TAAC-GFP fusion protein to chloroplasts in tobacco leaf protoplast, as revealed by confocal microscope imaging.** These are representative data of protoplasts that transiently expressed the fusion protein 24 h after electroporation. The *bars* represent 5 μm. *A*, differential interference contrast picture. *B*, GFP green fluorescence. *C*, Chl red autofluorescence. *D*, overlay of images *A*, *B*, and *C*.

For this purpose *Arabidopsis* chloroplast membrane subfractions, obtained by sucrose density gradient centrifugation, were analyzed by Western blotting using the anti-TAAC antibody and its preimmune serum. As shown in Fig. 3*A* (*upper panel*), a single band with M_r of 36.5 cross-reacted with the anti-TAAC antibody and corresponded to a chloroplast protein mainly located in the thylakoid membrane. The data do not, however, refute earlier findings (18), suggesting that this protein is also present in the envelope membrane. No cross-reaction was detected when the corresponding rabbit preimmune serum was used, further supporting the specificity of the anti-TAAC antibody (Fig. 3*A*, *upper panel*). The high purity of the analyzed thylakoid and envelope preparations was confirmed by Western blotting with antibodies against corresponding marker proteins, such as the thylakoid Lhcb2 protein, and the inner envelope TIC110 protein (Fig. 3*A*, *lower panels*).

Treatment with 1 M NaCl or 0.1% (w/v) Triton X-100 rendered the 36.5-kDa protein band in the membrane fraction, as in the case of control thylakoids (Fig. 3*B*). Only treatment with 1% (w/v) Triton X-100 solubilized the TAAC protein, indicating that this is a membrane-spanning protein and supporting the TMDs prediction data (Fig. 1).

The TAAC protein was immunolocalized on cryosections containing mesophyll cells of *Arabidopsis* rosette leaves, using serial dilutions of the TAAC antibody. Specific labeling was obtained at 1:50 dilution of the antibody. The analysis of several sections showed that the immunogold particles were mainly found in chloroplasts (Fig. 4). Particles were also occasionally

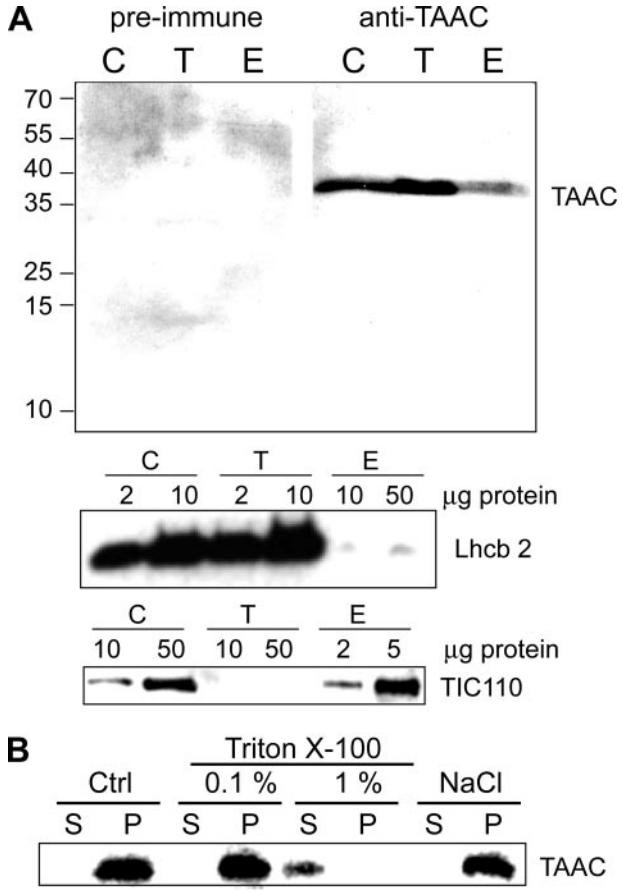

FIGURE 3. **Intra-chloroplast location of the TAAC protein in *Arabidopsis*.** *A*, Western blot analysis using preimmune and anti-TAAC antibodies was performed for protein extracts (30 μg/lane) from isolated chloroplasts (*C*), thylakoids (*T*), and envelope (*E*). The positions of the markers are shown on the *left*. The position of the TAAC protein (36.5 kDa) is indicated. As references, the distribution of Lhcb2 (thylakoid marker) and TIC110 (envelope marker) are shown. *B*, thylakoids were non-treated (Ctrl) or treated with 1 M NaCl and 0.1 or 1% (w/v) Triton X-100, and the distribution of the TAAC protein was analyzed by Western blotting in the corresponding supernatants (*S*) and pellets (*P*) (50 μg of protein/lane).

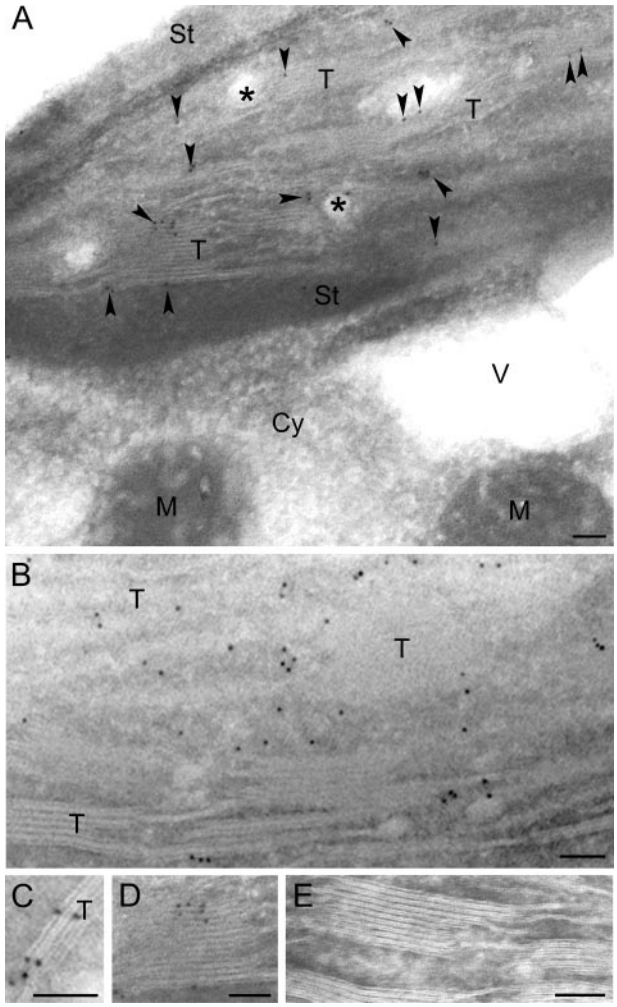

FIGURE 4. **Cryosections prepared from *Arabidopsis* leaf tissue were incubated with the anti-TAAC antibody followed by immunogold-labeled secondary antibody and electron microscope imaging.** The *bars* indicated in the figures represent 0.1 μm. *A*, gold particles (*arrows*) specifically labeled the chloroplast thylakoid membrane (*T*) and were absent in the soluble stroma (*St*), cytosol (*Cy*), mitochondria (*M*), and vacuole (*V*). *Asterisk*, plastoglobule. *B*, labeling of the thylakoid membrane system. *C*, labeling of the stroma-exposed regions is highlighted. *D*, few particles were observed within the grana stacks. *E*, control section (no anti-TAAC antibody) showed no labeling.

detected on peroxisomes (data not shown). The nucleus, cell wall, vacuole, cytosol, and organelles including mitochondria were not labeled (Fig. 4*A*). In chloroplasts the distribution of the immunogold particles, which reflects the distribution of the TAAC protein, was nonuniform. The particles were mostly associated with the stroma-exposed regions of the thylakoid membrane and of the grana stacks (Fig. 4, *B* and *C*), as also demonstrated for the chloroplast ATP synthase (35), and rarely associated with the stroma and envelope (Fig. 4*A*) or inside the grana stacks (Fig. 4*D*). Control sections, without primary antibodies, were not labeled (Fig. 4*E*). Taken together these studies demonstrate a chloroplast location for the TAAC protein, mainly in the thylakoid membrane.

Expression and Functional Characterization of the TAAC Protein in E. coli Cells—Sequence analyses data indicated adenine nucleotides as the most likely substrates for transport by TAAC (Fig. 1). To study its substrate specificity and kinetics for transport, we expressed a recombinant His_6-Xpress-TAAC-FLAG protein in *E. coli* cells. Fig. 5*A* shows a Western blot with Xpress antibody of protein extracts obtained by cell fractionation and at different steps of the purification process. A single cross-reacting band was detected in the IPTG-induced *E. coli* cells containing the *TAAC*-expressing plasmid (*pos.*) but not in the IPTG-induced cells lacking the coding sequence in the plasmid (*neg.*). The majority of the expressed TAAC protein was found in the membrane fraction (*M*), a finding not least important for the functional characterization in intact bacterial cells (see below). The TAAC protein was purified from the detergent-solubilized membrane protein extract by chromatography on a nickel column (M1) followed by a FLAG column (M2a). The TAAC protein was 3500- and 7000-fold enriched in M1 and M2a, respectively, compared with the crude membrane extract. The identity of the purified protein was confirmed by Western blotting with the anti-TAAC antibody (M2b) as well as by mass spectrometry analysis (data not shown). Coomassie staining revealed the TAAC protein as the main protein band in M2a sample, emphasizing the importance of this protein puri-

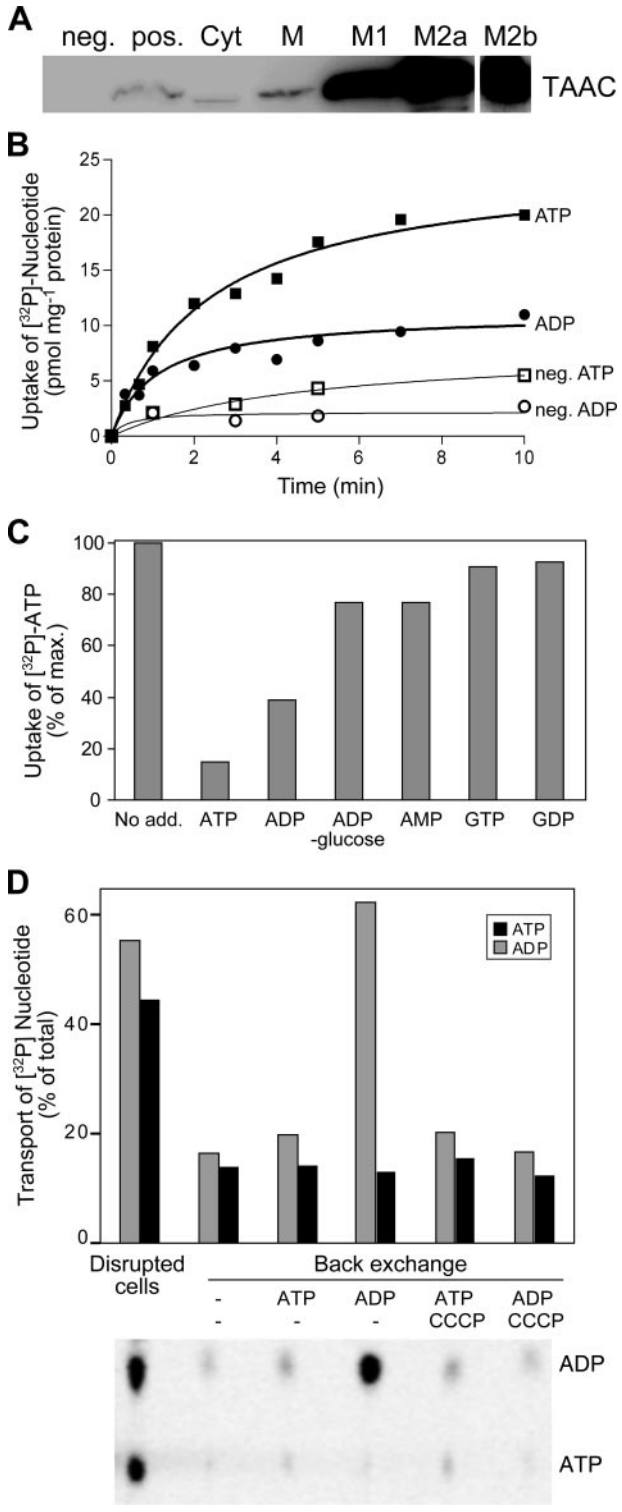

FIGURE 5. **Transport kinetics of the recombinant TAAC protein in *E. coli*.** *A*, *TAAC*-expressing (*pos.*) or non-expressing (*neg.*) *E. coli* cells were IPTG-induced for protein synthesis. Western blot analysis with Xpress antibodies was carried out for protein extracts obtained during subfractionation of *E. coli* cells (45 μg), cytosol (*Cyt*) and membrane (*M*) as well as during the two-step purification process (2 μg), eluate from the Ni-column (*M1*) and eluate from the FLAG column (*M2a*). Western blot with the anti-TAAC antibody of the second eluate (M2b) confirmed the identity of the recombinant protein. *B*, IPTG-induced TAAC-expressing cells were incubated with 50 μM [α-^{32}P]ATP (■) or [α-^{32}P]ADP (●) for the indicated periods of time. The uptake was terminated by rapid filtration. *C*, uptake of 50 μM [α-^{32}P]ATP was carried out in the presence of 2.5 mM nonlabeled nucleotides for 1 min. Values represent the percentage of remaining uptake compared with the value obtained in the absence of nonlabeled nucleotides. *D*, TAAC-expressing *E. coli* cells were preloaded with 50 μM [α-^{32}P]ATP followed by disruption or back exchange with buffer (−), 200 μM ATP or ADP in the absence or presence of 100 μM CCCP. After sedimentation and stopping of enzymatic activities, an aliquot of the supernatant was analyzed by TLC and phosphorimaging. *Upper panel*, plot of the amounts of exported nucleotides as a percentage of total radioactivity detected in the disrupted cells. *Lower panel*, representative phosphorimaged TLC plate used for quantification. The data presented in *panels B–D* are the mean of at least three independent experiments. S.E. < 10%.

fication system as a tool for crystallization and further characterization.

Fig. 5*B* shows a time dependence for the uptake of [α-^{32}P]ATP and [α-^{32}P]ADP into intact *E. coli* cells expressing the recombinant TAAC protein. In the background, non-time-dependent binding of nucleotides was observed in IPTG-treated cells lacking the *TAAC* insert, representing a maximum of 19 and 23% of the assayed uptake of ATP and ADP, respectively. Furthermore, radioactive nucleotides were detected in washed and disrupted expressing cells (see Fig. 4*D*) but not in the control cells (data not shown), indicating that the assayed transport activity is dependent on the presence of the TAAC protein. The ratio of ATP to ADP uptake was about 2.2, suggesting a preferred import of ATP *versus* ADP into *E. coli* cells. This is opposite to the preferred import of ADP *versus* ATP by heterologously expressed *Arabidopsis* mitochondrial AACs (17).

For determination of the K_m and V_{max} values of the TAAC-catalyzed transport, the *E. coli* cells were incubated with 0–250 μM radioactive adenine nucleotides for 1 min (supplemental Fig. S2). The apparent K_m values for ATP and ADP (supplemental Table S1) were about 45 μM, *i.e.* intermediate between those reported for *Arabidopsis* (10–15 μM) and mammalian (100–150 μM) AACs when expressed and assayed in *E. coli* cells (17). The calculated V_{max} value for ATP and ADP uptake were 0.71 and 0.53 nmol mg^{-1} protein h^{-1} (supplemental Table S1). Both V_{max} values are in the same range as those determined for the *Arabidopsis* mitochondrial AACs expressed in *E. coli*, *i.e.* 0.18–4.41 nmol mg^{-1} protein h^{-1} (17).

The presence of CCCP increased the apparent K_m value of TAAC for ATP to 170 μM and the corresponding V_{max} value to 1.79 nmol mg^{-1} protein h^{-1} (supplemental Fig. S2 and Table S1). The corresponding values for ADP were not affected by the presence of CCCP. The fact that TAAC has a lower affinity for binding ATP in non-energized *E. coli* membranes could be due to a protein conformational change such that the substrate becomes loosely bound and is faster released on the other side of the membrane. The K_m values were only slightly lowered by CCCP in the case of the mitochondrial AACs expressed in *E. coli* (17). The mechanistic reason for this discrepancy with respect to CCCP is not known. Nevertheless, the TAAC transport activity shows other differences as well. For example, export of ADP by TAAC is inhibited by CCCP (see below), at variance with the same activity performed by the mitochondrial AACs (17).

To investigate the nucleotide transport specificity of TAAC, we performed uptake of [α-^{32}P]ATP into *E. coli* cells expressing the recombinant protein in the presence of excess of various nonlabeled nucleotides (Fig. 5*C*). In comparison with the con-

trol uptake, ATP competed with the highest efficiency (83%) closely followed by ADP (60%). The guanine nucleotides did not affect the ATP uptake, suggesting that although they could bind to the carrier protein (10), they are not substrates for transport. ADP-glucose (Fig. 5*C*) and phosphate (data not shown) did not compete with the ATP uptake, indicating that TAAC is not involved in neither nucleotide-sugar nor phosphate transport. The competition data strongly support that *Arabidopsis* TAAC specifically transports adenine nucleotides, as reported for mammalian AACs, and in contrast to maize AAC, which can also transport guanine nucleotides (Ref. 36 and references therein).

Most MCF members catalyze strict solute exchange reactions. *TAAC*-expressing *E. coli* cells were preloaded with [α-^{32}P]ATP followed by back exchange with nonlabeled external substrates, and the released nucleotides were separated by thin layer chromatography (TLC). As shown in Fig. 5*D*, disrupted preloaded cells contained both radioactive ATP and ADP, indicating that an uptake of ATP had taken place and that part of it was converted to ADP in the cytosol. No significant amount of radioactive nucleotides was released after the addition of buffer. A preferential export of [α-^{32}P]ADP occurred during the back exchange with externally added adenine nucleotides and was effectively inhibited by CCCP (Fig. 5*D*).

In Planta Functional Analyses of the TAAC Protein—The nucleotide uptake and exchange data obtained from functional expression of the recombinant TAAC in *E. coli* were compared with those in *Arabidopsis* thylakoids. All experiments using thylakoids were carried out in darkness when ATP binding and hydrolysis by the catalytic portion (CF1) of the ATP synthase is extremely low (Refs. 37 and 38 and references therein). Under our experimental conditions, the uptake of [α-^{32}P]ATP into thylakoids had a fast linear phase (up to 1 min) and reached a plateau level of 150 pmol of ATP/mg Chl within about 5 min (supplemental Fig. S3*A*). The estimated apparent K_m for ATP was about 0.5 μM, (supplemental Fig. S3B), *i.e.* a significantly lower value than the K_m of the recombinant TAAC as determined in *E. coli* (47 μM, supplemental Table S1). Another difference from TAAC-mediated transport in *E. coli* is that, in addition to ATP and ADP, GDP also competed with the uptake of [α-^{32}P]ATP in thylakoids (supplemental Fig. S3C). These data imply that, in addition to TAAC, there exist other sites for ATP binding and transport in thylakoids, including the previously characterized binding to the ATP synthase (37, 39, 40). Nevertheless, our data also indicate similar kinetics to the ones reported for nucleotide uptake (by AACs) in isolated mitochondria (17, 41).

To investigate the internal affinities of thylakoids for adenine nucleotides, we carried out back exchange experiments in thylakoids preloaded with [α-^{32}P]ATP (supplemental Fig. S3*D*). Preloaded thylakoids contained radioactive ATP and ADP in a ratio of about 4:1 and showed a preferential export of [α-^{32}P]ADP, supporting the data obtained for TAAC in *E. coli* cells (Fig. 5*D*). Because incubation with ADP is known to abolish the ATPase activity of CF1 (38), its interference in the observed exchange is not very likely. The fact that even GDP induced export of ADP (supplemental Fig. S3*D*) has significance for the previously characterized NDPK activity in the thylakoid lumen (10). Because GDP competed with ATP uptake and induced ADP export, there must exist another transport system than TAAC for GDP in thylakoids.

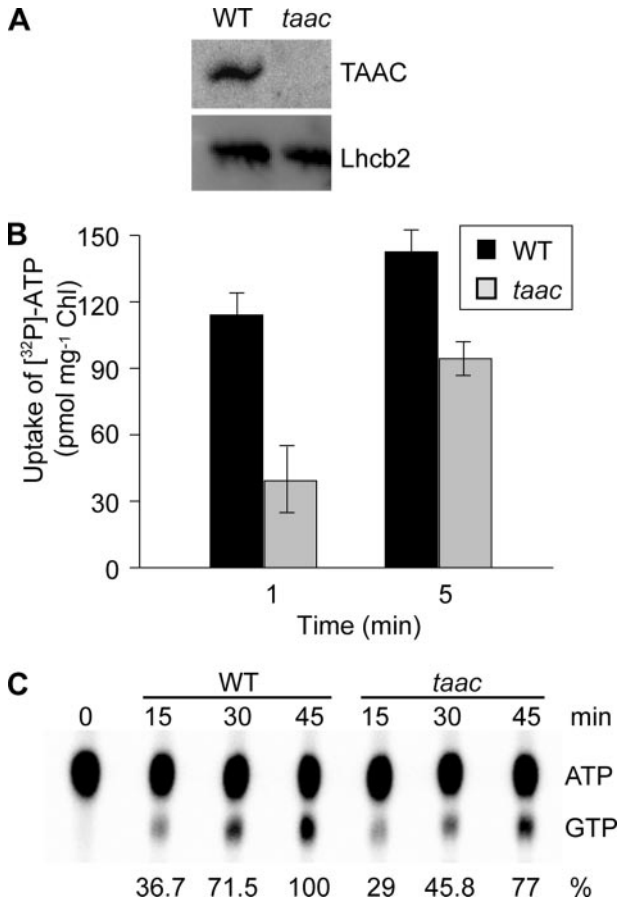

FIGURE 6. **Functional characterization of an *Arabidopsis TAAC* knock-out mutant.** *A*, thylakoids were isolated from the *taac* mutant and WT plants and analyzed by Western blotting with anti-TAAC (30 μg of protein/lane) and anti-Lhcb2 (1 μg of protein/lane) antibodies. *B*, thylakoids were incubated in darkness with 10 μM [α-^{32}P]ATP for 1 or 5 min and washed, and the bound radioactivity was counted by scintillation. *C*, thylakoids were incubated with 1 mM [γ-^{32}P]ATP and 1 mM GDP for the indicated periods of time, and the nucleotides were analyzed by TLC followed and phosphorimaging.

To determine the physiological influence of TAAC on the availability of adenine nucleotides inside the chloroplast thylakoid lumen, a FLAG line with a T-DNA insertion in the *TAAC* gene (*taac* mutant, supplemental Fig. S1*A*) was analyzed and compared with WT. The homozygoty of this line was confirmed by PCR (supplemental Fig. S1*B*), and the lack of TAAC was verified by Western blotting of isolated thylakoids (Fig. 6*A*). As a control the amount of Lhcb2 was analyzed and shown to be at comparable levels in the WT and the *taac* mutant. Uptake of [α-^{32}P]ATP into dark-incubated thylakoids isolated from the *taac* mutant was reduced to 37% (at 1 min) and 68% (at 5 min) of the WT levels (Fig. 6*B*). Interconversion of ATP to GTP in the thylakoids (via lumenal NDPK3) was reduced to 60–70% of the WT levels (Fig. 6*C*). Additional phenotypic effects of *TAAC* disruption included about 40% reduction in the thylakoid content as compared with WT (expressed as mg Chl/g of leaf, supplemental Fig. S4), resulting in pale green leaves of the *taac* mutant.

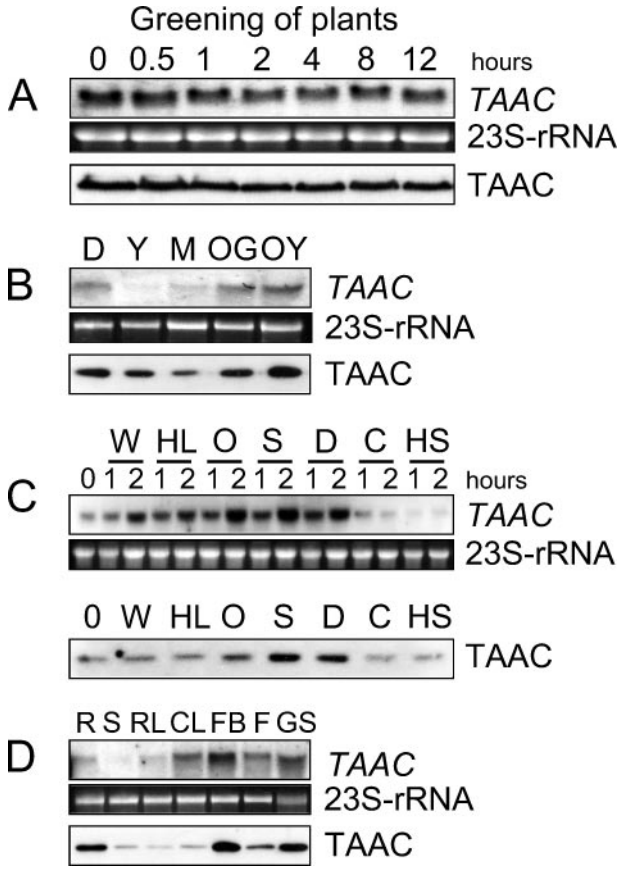

FIGURE 7. **TAAC expression pattern in *Arabidopsis*.** The total RNA (5–10 μg) was isolated, and expression of the *TAAC* transcript was investigated by Northern blotting. As a reference, the 23 S rRNA (ribosomal RNA) pattern in the gel was visualized by staining with ethidium bromide. The corresponding total protein extracts (15 μg) were analyzed by Western blotting with the anti-TAAC antibody. *A*, *Arabidopsis* seedlings were grown on liquid Murashige Skoog media for 10 days in darkness and then illuminated with 50 μmol of photons m^{-2} s^{-1} for the indicated periods of time. *B*, leaves at various developmental stages: *D*, developing; *Y*, young; *M*, mature fully developed; *OG*, old still green; *OY*, senescent yellow. *C*, detached leaves were exposed for 0, 1, or 2 h to various stress conditions: wounding stress (*W*), cut into 1 cm^2 segments; high light stress (*HL*), floated on water and illuminated with 1000 μmol of photons m^{-2} s^{-1}; oxidative stress (*O*), incubated in 2% H_2O_2 solution; salt stress (*S*), incubated in 0.4 M NaCl solution; desiccation stress (*D*), kept on Whatman paper at room temperature; cold stress (*C*), detached leaves were floated on water at 4 °C; heat shock (*HS*), floated on water at 42 °C. *D*, various plant organs: *R*, roots; *S*, stems; *RL*, rosette leaves; *CL*, cauline leaves; *FB*, flower buds; *F*, flowers; *GS*, green siliques.

TAAC Expression Pattern in Arabidopsis—To get information about the *in planta* role of TAAC, we addressed several questions; whether expression of the *TAAC* gene in *Arabidopsis* is restricted to photosynthetic tissues and whether it occurs at specific stages of development and/or under certain stress conditions. As shown by Northern blot experiments (Fig. 7*A*) a significant amount of *TAAC* transcript was detected in seedlings grown in darkness, and its level did not change significantly during a period of up to 12 h of greening. The level of the TAAC protein in the corresponding protein extracts followed the transcript pattern, as revealed by Western blotting with the anti-TAAC antibody (Fig. 7*A*). For comparison, the transcription of maize mitochondrial AACs readily occurs in darkness, and decreases as soon as the tissue becomes photosynthetically active (Ref. 36 and references therein).

We also investigated expression during various leaf developmental stages (Fig. 7*B*). Our data revealed that the amount of the *TAAC* transcript was high in developing leaves, decreased during maturation, and increased again during senescence to levels exceeding those present in developing leaves. The TAAC level in the corresponding protein extracts generally followed the level of corresponding transcripts. Next, we assayed expression in leaves exposed to various abiotic stress conditions (Fig. 7*C*). Although the amounts of the *TAAC* transcript were increased during wounding, light stress, oxidative stress, salt stress, and desiccation, a drastic reduction was detected under heat shock conditions. Similarly, the exposure of leaves to low temperature led to a slight decrease in the *TAAC* transcript level. As before, the protein pattern resembled the one of the transcript. Finally, the *TAAC* expression was investigated in various *Arabidopsis* organs (Fig. 7*D*). The highest levels of *TAAC* transcript and protein were detected in developing photosynthetic organs such as leaves (see also Fig. 7*B*), flower buds, and green siliques followed by fully developed organs such as roots, flowers, cauline and rosette leaves, and least in the stem. For comparison, the mitochondrial AACs show a similar expression pattern in all tissues (36), pointing to a more general role in plant metabolism. High TAAC levels in *Arabidopsis* dark-grown seedlings in developing and senescent leaves may have relevance for initiation of biogenesis and turnover of the photosynthetic apparatus in the thylakoid membrane.

DISCUSSION

The old dogma was that mitochondria and plastids have different types of nucleotide transporters, namely mitochondrial AACs that export ATP to the cytosol, and plastidic NTTs that perform ATP uptake into the stroma (42). The data presented in this work demonstrate that the chloroplast thylakoid membrane contains an MCF member, namely an ATP/ADP carrier, herein named TAAC. We identified this protein in *Arabidopsis* thylakoids as the product of the At5g01500 gene. Detection of the TAAC protein in low amounts in the chloroplast envelope and in non-photosynthetic plastids points to an apparent dual localization. We show that the recombinant TAAC protein is specific for adenine nucleotide transport and imports ATP in exchange for ADP across the *E. coli* cytoplasmic membrane. The same exchange pattern occurs across *Arabidopsis* thylakoids. Finally, we show reduction of ATP transport and metabolism within the thylakoid membrane in a *TAAC* knock-out mutant.

Among photosynthetic organisms, ESTs from the green alga *Chlamydomonas reinhardtii*, maize, rice, wheat, potato, and soybean show 60–80% identity to the *Arabidopsis TAAC* gene sequence, as revealed by orthologues search in TIGR databases. No homologues in the genome data base of cyanobacteria (Cyanobase) were found, supporting a previous bioinformatic report which suggested that MCFs are a later addition during the development of the eukaryotic cell (43).

Arabidopsis TAAC possesses the characteristic sequence features of MCF and AAC members (Fig. 1). Measurements of radioactive adenine nucleotide transport across *E. coli* membrane demonstrated that this protein is indeed an AAC, sharing similarities with but also differences from the mitochondrial

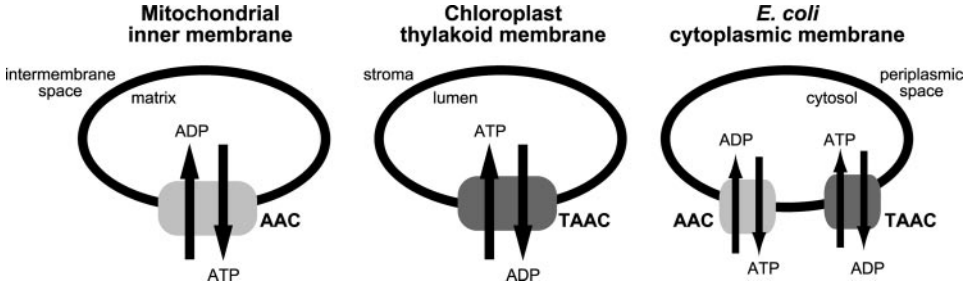

FIGURE 8. **Schematic model of adenine nucleotide exchange mediated by AAC and TAAC.** The native and recombinant AAC proteins export endogenously synthesized ATP and import external ADP into mitochondria and *E. coli* cells, respectively, as indicated by previous uptake and back exchange experiments (17, 41). The native TAAC transports stromal ATP into the thylakoid lumen (Ref. 10 and supplemental Fig. S3). The recombinant TAAC protein transports external ATP in exchange for cytosolic ADP across *E. coli* membrane (Fig. 5). Thus, the direction of adenine nucleotide exchange by the recombinant AAC and TAAC across *E. coli* membrane is similar to the direction of transport by the native proteins across the mitochondrial and thylakoid membrane, respectively.

homologues. The most striking difference is the ATP/ADP counter exchange catalyzed by TAAC (Fig. 5), which is opposite to ADP/ATP exchange by AAC across *E. coli* membrane (17). The pattern of adenine nucleotide exchange for both TAAC and AAC *in organello* is similar to the one obtained for the corresponding recombinant proteins expressed in *E. coli* but apparently opposite to each other (Fig. 8). The explanation resides in the fact that, structurally, the thylakoid membrane and its lumenal space represent intra-chloroplast compartments without correspondent in mitochondria. Nevertheless, the translocation of adenine nucleotides by TAAC and AAC proceeds in an analogous manner across thylakoid and mitochondrial inner membrane, namely from the site of ATP synthesis (stromal or matrix side) to the other side of the membrane (thylakoid lumen or mitochondrial intermembrane space) (Fig. 8).

There is a lot of information available for the adenine nucleotide transport system in mitochondria and about the activities of recombinant AACs (17, 41), which could be compared with the uptake data for thylakoid membrane and recombinant TAAC (this work). In the past nucleotide binding to the thylakoid membrane has been mainly attributed to the ATP synthase. It was shown to readily occur in darkness and to increase at least 3-fold during photophosphorylation (37, 39, 40). Remarkably, uncouplers and inhibitors of photophosphorylation were found effective in suppressing the binding in the light but not the one observed in darkness (37). Using radioactive azido-ATP labeling of thylakoids, it later demonstrated specific binding to a nucleotide carrier of 36.5 kDa (10), identified as a TAAC in this work. Therefore, we suggest that the TAAC-catalyzed uptake of ATP into thylakoids in darkness is a component of the previously reported tight ATP binding (37). ATP uptake in mitochondria (17, 41) and ATP binding to thylakoids in darkness (37) are both largely unaffected by uncouplers and inhibitors of oxidative/photo phosphorylation, indicating that a protonmotive force across the membrane is not absolutely required. In light of the novel concept of induced transition fit proposed to function in transport catalysis (44), it is the interaction of the nucleotide substrate with the carrier providing the catalytic energy for transport. Nevertheless, external energy may maximize the transition fit; hence, the transport efficiency.

Data available in public microarrays collections, such as Genevestigator data base (45), indicated the highest levels of *TAAC* transcript in seeds followed by shoot apex and much lower similar levels in other tissues (flowers, roots, and rosette leaves). The same microarray data indicated high transcript levels in young leaves and petiole and low levels in senescent leaves. Our data show a different pattern, with the highest expression detected in dark-grown seedlings, developing green tissues (leaves, flower buds, siliques), and senescent leaves (Fig. 7). Expression in roots and flowers indicates the presence of the TAAC protein even in non-green plastids. Developing plastids, etioplasts, and to a lower extent also other types of plastids have in addition to envelope internal membranes that could convert to thylakoid membranes upon illumination (3). At least in developing plastids, the internal membranes are occasionally continuous with the envelope (3).

The TAAC protein is found readily expressed in dark-grown seedlings and should be very active during biogenesis of the photosynthetic apparatus, which starts only a few minutes after light exposure (46). The HCF136 protein is also produced in dark-grown seedlings and is kept at a stable level during light-induced greening (47). This protein was demonstrated to be located in the thylakoid membrane and must be present when PSII complexes are made in the stroma regions. Similarly to the HCF136 protein, TAAC has to be present before or at least concomitantly with the accumulation of photosynthetic complexes. It may supply various biosynthetic processes with ATP, which was shown to be produced in increasing amounts during embryonic photosynthesis (48).

In leaf chloroplasts, TAAC was detected mainly in the thylakoid but also in the envelope fraction to a lower extent (Fig. 3). Because a previous proteomic work (18) has identified TAAC in purified envelope preparations, one cannot exclude its presence also in the envelope. The localization of another MCF member in both mitochondria and chloroplast envelope has recently been reported (49). Furthermore, there are several examples of proteins involved in Chl synthesis, thylakoid biogenesis, and chloroplast morphology targeted to both envelope and thylakoid membranes (50–52) that support our findings. What does a dual localization of TAAC mean? The level of TAAC transcript and protein peaked in young green tissues that undergo rapid plastid development and declined as the plant matured (Fig. 7). Furthermore, the thylakoid membrane was the predominant location under conditions in which mature tissues were used as a source of chloroplasts (Figs. 3 and 4). These observations imply that TAAC is needed to be present in the internal membranes of developing plastids more than in the thylakoids of mature chloroplasts. Its location depends on the developmental stage of plastids, and TAAC may have multiple functions. In premature chloroplasts it may be initially located in the envelope and participate in the development of

internal membranes into thylakoid membranes. In contrast, in mature chloroplasts TAAC is mainly located in the thylakoid membrane and may have a role in its turnover.

We also detect increasing *TAAC* transcript levels under senescence and various abiotic stress treatments of leaves, in contrast to the Genevestigator data base reporting down-regulation and no change, respectively. We suggest a role for TAAC in supplying ATP into the thylakoid lumen for mobilization of N-resources (during senescence), for refolding of misfolded thylakoid proteins (during import), and for their degradation (during stress). Alternatively, it is converted to GTP in the thylakoid lumen (10), which via binding and hydrolysis by the extrinsic PsbO subunit of PSII complex stimulates the light-induced degradation of the reaction center D1 protein in plants (26, 53).

To our knowledge the product of the At5g01500 gene is the first chloroplast AAC identified and characterized at tissue, cellular, and molecular levels. The TAAC protein represents a link between ATP synthesis on the stromal side of the thylakoid membrane and nucleotide-dependent reactions in the lumenal space (10, 12, 13). Failure to detect a more substantial reduction of ATP transport and metabolism in the *taac* mutant suggests that the At5g01500 gene may encode a transporter that normally contributes only 30–40% to the thylakoid transport. As an alternative, TAAC may quantitatively be a major player, and other yet unidentified transporters partially compensate for its disruption in the *taac* mutant.

Although further analyses are required to elucidate the physiological role of this carrier, it should be noted that other compounds resulting from nucleotide metabolism such as phosphate cannot be exported by TAAC, because it is not a substrate of this carrier, implying the presence of another transporter(s) responsible for its removal. The identification of these proteins should be the focus of further studies aimed at understanding the lumenal network of nucleotide metabolism.

Acknowledgments—We thank Prof. G. von Heijne (Stockholm University) for helpful suggestions and discussions of the TAAC prediction data, Prof. J. Soll (Munich University) for providing the anti-TIC110 antibody, and Kent Lundh (Kalmar University) for help with the chromatographic techniques. The Ecker size-selected Arabidopsis cDNA library (CD4–14) provided by the Arabidopsis Biological Resource Center at Ohio State University is acknowledged. We thank the Institut National de la Recherche Agronomique (Station de génétique, Versailles, France) for providing the FLAG 443D03 Arabidopsis line.

REFERENCES

1. Ephritikhine, G., Ferro, M., and Rolland, N. (2004) *Plant Physiol. Biochem.* **42,** 943–962
2. van Wijk, K. J. (2004) *Plant Physiol. Biochem.* **42,** 963–977
3. Vothknecht, U. C., and Westhoff, P. (2001) *Biochim. Biophys. Acta* **1541,** 91–101
4. van Wijk, K. J. (2001) in *Regulation of Photosynthesis* (Aro, E. M., and Andersson, B., eds) pp. 153–175, Kluwer Academic Publishers Group, Dordrecht, Netherlands
5. Ettinger, W. F., Clear, A. M., Fanning, K. J., and Peck, M. L. (1999) *Plant Physiol.* **119,** 1379–1386
6. Shingles, R., Wimmers, L. E., and McCarty, R. E. (2004) *Plant Physiol.* **135,** 145–151
7. Vambutas, V., Tamir, H., and Beattie, D. S. (1994) *Arch. Biochem. Biophys.* **312,** 401–406
8. Hinnah, S. C., and Wagner, R. (1998) *Eur. J. Biochem.* **253,** 606–613
9. Pottosin, I. I., and Schonknecht, G. (1996) *J. Membr. Biol.* **152,** 223–233
10. Spetea, C., Hundal, T., Lundin, B., Heddad, M., Adamska, I., and Andersson, B. (2004) *Proc. Natl. Acad. Sci. U. S. A.* **101,** 1409–1414
11. Abdel-Ghany, S. E., Muller-Moule, P., Niyogi, K. K., Pilon, M., and Shikanai, T. (2005) *Plant Cell* **17,** 1233–1251
12. Wagner, V., Gessner, G., Heiland, I., Kaminski, M., Hawat, S., Scheffler, K., and Mittag, M. (2006) *Eukaryot. Cell* **5,** 457–468
13. Rinalducci, S., Larsen, M. R., Mohammed, S., and Zolla, L. (2006) *J. Proteome Res.* **5,** 973–982
14. Pebay-Peyroula, E., Dahout-Gonzalez, C., Kahn, R., Trezeguet, V., Lauquin, G. J., and Brandolin, G. (2003) *Nature* **426,** 39–44
15. Millar, A. H., and Heazlewood, J. L. (2003) *Plant Physiol.* **131,** 443–453
16. Heazlewood, J. L., Tonti-Filippini, J. S., Gout, A. M., Day, D. A., Whelan, J., and Millar, A. H. (2004) *Plant Cell* **16,** 241–256
17. Haferkamp, I., Hackstein, J. H. P., Voncken, F. G. J., Schmit, G., and Tjaden, J. (2002) *Eur. J. Biochem.* **269,** 3172–3181
18. Ferro, M., Salvi, D., Brugiere, S., Miras, S., Kowalski, S., Louwagie, M., Garin, J., Joyard, J., and Rolland, N. (2003) *Mol. Cell. Proteomics* **2,** 325–345
19. Norén, H., Svensson, P., and Andersson, B. (2004) *Physiol. Plant.* **121,** 343–348
20. Ginalski, K., Elofsson, A., Fischer, D., and Rychlewski, L. (2003) *Bioinformatics* **19,** 1015–1018
21. Schwede, T., Kopp, J., Guex, N., and Peitsch, M. C. (2003) *Nucleic Acids Res.* **31,** 3381–3385
22. Kieber, J. J., Rothenberg, M., Roman, G., Feldmann, K. A., and Ecker, J. R. (1993) *Cell* **72,** 427–441
23. Eshaghi, S., Andersson, B., and Barber, J. (1999) *FEBS Lett.* **446,** 23–26
24. Bradford, M. M. (1976) *Anal. Biochem.* **72,** 248–254
25. Porra, R. J., Thompson, W. A., and Kriedemann, P. E. (1989) *Biochim. Biophys. Acta* **975,** 384–394
26. Spetea, C., Hundal, T., Lohmann, F., and Andersson, B. (1999) *Proc. Natl. Acad. Sci. U. S. A.* **96,** 6547–6552
27. Tokuyasu, K. T. (1980) *Histochem. J.* **12,** 381–403
28. Sambrook, J., Fritsch, E. F., and Maniatis, T. (1989) *Molecular Cloning: A Laboratory Manual*, 2nd Ed., Cold Spring Harbor Laboratory Press, Cold Spring Harbor
29. Lagerstedt, J. O., Voss, J. C., Wieslander, A., and Persson, B. L. (2004) *FEBS Lett.* **578,** 262–268
30. Tjaden, J., Schwoppe, C., Mohlmann, T., Quick, P. W., and Neuhaus, H. E. (1998) *J. Biol. Chem.* **273,** 9630–9636
31. Weber, A. P., Schwacke, R., and Flugge, U. I. (2005) *Annu. Rev. Plant Biol.* **56,** 133–164
32. Sun, Q., Emanuelsson, O., and van Wijk, K. J. (2004) *Plant Physiol.* **135,** 723–734
33. Kleffmann, T., Russenberger, D., von Zychlinski, A., Christopher, W., Sjolander, K., Gruissem, W., and Baginsky, S. (2004) *Curr. Biol.* **14,** 354–362
34. Nury, H., Dahout-Gonzalez, C., Trezeguet, V., Lauquin, G. J., Brandolin, G., and Pebay-Peyroula, E. (2006) *Annu. Rev. Biochem.* **75,** 713–741
35. Anderson, J. M., and Andersson, B. (1982) *Trends Biochem. Sci.* **7,** 288–292
36. Laloi, M. (1999) *Cell. Mol. Life Sci.* **56,** 918–944
37. Magnusson, R. P., and McCarty, R. E. (1976) *J. Biol. Chem.* **251,** 7417–7422
38. McCarty, R. E. (2005) *J. Bioenerg. Biomembr.* **37,** 289–297
39. Smith, D. J., and Boyer, P. D. (1976) *Proc. Natl. Acad. Sci. U. S. A.* **73,** 4314–4318
40. Abbott, M. S., Czarnecki, J. J., and Selman, B. R. (1984) *J. Biol. Chem.* **259,** 12271–12278
41. Winkler, H. H., Bygrave, F. L., and Lehninger, A. L. (1968) *J. Biol. Chem.* **243,** 20–28
42. Winkler, H. H., and Neuhaus, H. E. (1999) *Trends Biochem. Sci.* **24,** 64–68
43. Kunji, E. R. (2004) *FEBS Lett.* **564,** 239–244
44. Klingenberg, M. (2006) *Biochim. Biophys. Acta* **1757,** 1229–1236
45. Zimmermann, P., Hirsch-Hoffmann, M., Hennig, L., and Gruissem, W.

(2004) *Plant Physiol.* **136,** 2621–2632
46. Bertrand, M., Bereza, B., and Dujardin, E. (1988) *Z. Naturforsch.* **43,** 443–448
47. Meurer, J., Plucken, H., Kowallik, K. V., and Westhoff, P. (1998) *EMBO J.* **17,** 5286–5297
48. Borisjuk, L., Rolletschek, H., Radchuk, R., Weschke, W., Wobus, U., and Weber, H. (2004) *Plant Biol.* (*Stuttg*) **6,** 375–386
49. Palmieri, L., Arrigoni, R., Blanco, E., Carrari, F., Zanor, M. I., Studart-Guimareas, C., Fernie, A. R., and Palmieri, F. (2006) *Plant Physiol.* **142,** 855–865
50. Che, F. S., Watanabe, N., Iwano, M., Inokuchi, H., Takayama, S., Yoshida, S., and Isogai, A. (2000) *Plant Physiol.* **124,** 59–70
51. Inoue, K., Baldwin, A. J., Shipman, R. L., Matsui, K., Theg, S. M., and Ohme-Takagi, M. (2005) *J. Cell Biol.* **171,** 425–430
52. Gao, H., Sage, T. L., and Osteryoung, K. W. (2006) *Proc. Natl. Acad. Sci. U. S. A.* **103,** 6759–6764
53. Lundin, B., Thuswaldner, S., Shutova, T., Eshaghi, S., Samuelsson, G., Barber, J., Andersson, B., and Spetea, C. (2006) *Biochim. Biophys. Acta* 10.1016/j.bbabio.2006.10.009